Available online at www.sciencedirect.com
SCIENCE DIRECT®
International Journal of Solids and Structures 41 (2004) 6383–6405
INTERNATIONAL JOURNAL OF SOLIDS and STRUCTURES
www.elsevier.com/locate/ijsolstr

A computational strategy for the random response of assemblies of structures

C. Blanzé *, L. Champaney

LMT Cachan, ENS de Cachan/CNRS/PARIS VI, 61, av. du Pt Wilson, F94235 Cachan Cedex, France

Received 27 October 2003; received in revised form 29 April 2004
Available online 10 June 2004

Abstract

This paper presents a dedicated approach to the calculation of the random response of assemblies with uncertain interface characteristics. The random response is constructed using a polynomial chaos expansion (PCE). A decomposition of the assemblies into substructures and interfaces is defined and associated with a dedicated computational strategy which leads to a local/global algorithm enabling the treatments of the substructure and of the interface problems to be uncoupled. Since the only uncertain parameters are those which appear in the interface equations, this approach results in a drastic reduction of the computational costs. This paper first presents the classical stochastic finite element strategy for this kind of problem, then details the proposed dedicated approach. The applications concern structures assembled with uncertain elastic bonded joints. The proposed approach is compared to the Monte Carlo method and to the stochastic finite element method.

Keywords: Assemblies; Uncertainties; Probabilistic mechanics; Polynomial chaos; LATIN method

1. Introduction

Finite element calculations of structural assemblies are being used more and more in the industrial world (Blanzé et al., 2000). The recent progress in industrial finite element codes associated with the efficiency of modern computers enable one to carry out increasingly detailed calculations on individual parts of an assembly. It has become possible to take into account very complex geometries and material behavior. Nevertheless, a critical aspect of such calculations is the modeling of the boundary conditions. Therefore, it is necessary to calculate complete assemblies. Thus, the boundary condition problem is replaced by the problem of modeling the mechanical behavior of the connections between structural parts. These interactions between parts are often modeled by means of interface entities. Models of interface behavior have been developed for contact, friction, joints, adhesives (Ladevèze et al., 2000)... The identification of the

* Corresponding author. Tel.: +33-1-47-40-21-86; fax: +33-1-47-40-22-40.
E-mail addresses: claude.blanze@lmt.ens-cachan.fr, blanze@lmt.ens-cachan.fr (C. Blanzé), laurent.champaney@lmt.ens-cachan.fr (L. Champaney).

0020-7683/$ - see front matter © 2004 Elsevier Ltd. All rights reserved.
doi:10.1016/j.ijsolstr.2004.05.003

mechanical parameters of an interface's behavior (stiffness and friction coefficients, fracture energies, ...) is a complicated task because one cannot perform experimental tests on a single interface: these are always performed on a simple assembly containing the interface. Thus, the identification process must assume complete knowledge of the rest of the assembly and is very often coupled with numerical calculations. Consequently, considerable uncertainties can affect the mechanical parameters measured (Tong and Steven, 1999; Van Straalen et al., 1998). Moreover, in industrial applications where classical joining techniques (bolts, rivets, ...) are not possible, using adhesive techniques is of a great interest (examples: joining of peaces of aircraft fuselage, connection of tubular structures ...). In such situations, controlling the adhesively bonded joints parameters (thickness of the joint, stiffness and quality of the adhesive, ...) is very difficult and this can lead to a great uncertainty on the response on the joints.

The aim of the work presented here is to propose an efficient approach for the prediction of the random response of an assembly when significant uncertainties affect the parameters of the connections.

Starting with the assumption that the material properties of a particular interface can be modeled within the framework of probability theory, a very rich mathematical background is available to completely characterize the probabilistic behavior and evolution of the structure under external perturbations. Thus, the treatment presented in this paper adheres to a probabilistic framework. The theory is based on the L_2 properties of second-order random variables and the possibility of treating these variables as elements of a particular Hilbert space (Wiener, 1938; Loeve, 1977; Ghanem, 1999). Effective analytical methods for stochastic non-linear systems are applicable only in some simple cases. When dealing with more complex systems, approximate methods and numerical integration are necessary. If the uncertainties are small, perturbation theory is a very valuable tool for analyzing their effects (Kleiber and Hien, 1992). If they are larger, then perturbation theory is not applicable. One obvious way to deal with stochastic partial differential equations (SPDEs) is the Monte Carlo method. This is an expensive technique, especially if some higher-order accuracy is sought for the mean values, standard variations, queues of distributions, etc. Various numerical methods for solving SPDEs have been proposed in the literature (Ghanem and Kruger, 1996). Ghanem and Spanos (1991) and Ghanem (1999) advocate a hybrid finite element and spectral approach, which we will refer to as the spectral stochastic finite element method (SSFEM), while the monograph by Kleiber and Hien (1992) uses aperturbation approach. Elishakoff and Ren (1999) examine engineering finite element methods for structures with large stochastic variations and point to limitations in some of the approaches. Deb et al. (2001) present a theory of a posteriori error estimation and corresponding adaptive approaches. More complete descriptions of works on computational methods for SPDEs used to model stochastic behavior in mechanical problems can be found in the books by Kleiber and Hien (1992) and Ghanem and Spanos (1991). Review articles were written by Vanmarcke (1983), Lin et al. (1986), Vanmarcke et al. (1988) and Matthies et al. (1997). The application of the spectral stochastic finite element method (SSFEM) for the analysis of randomly fluctuating properties of an interface between two elastic media was addressed by Ghanem and Brzakala (1996) and concern a geotechnical application.

Our computational strategy to solve the problem is based on the LATIN method. This method is a general strategy which was developed initially for the analysis of non-linear structural problems (Ladevèze, 1999). It has been successfully extended to the calculation of assemblies of structures involving many types of connections (Blanzé et al., 1995, 2000; Ladevèze et al., 2000). In order to deal with such problems, the technique is associated with a decomposition of the problem into substructures and interfaces. The LATIN method is based on a decomposition of the problem into local, possibly non-linear, equations describing the behavior of the interfaces and linear equations expressing the global equilibrium. Thus, since the only uncertain parameters reside in the local equations of the behavior at the interfaces, this strategy results in the treatment of the uncertainties and the treatment of the global problem being uncoupled.

In the following sections, the reference problem for a decomposition of an assembly into substructures and interfaces will be presented first. The classical stochastic finite element procedure in which interface

finite elements are used to model the connection will be described. Then, the proposed approach will be developed for the case of uncertain elastic behavior at the interfaces. A comparison of the Monte Carlo method, the SSFEM and our iterative approach will be shown for a simple one-dimensional example. Finally, a two-dimensional industrial example comprising two adhesively bonded joints will be presented.

2. The reference problem

Here, we are considering structural assembly problems in which both the behavior of the components and the external loads are deterministic. The randomness of the response comes from the random behavior of the connections. In general, random uncertainties are modeled using a parametric approach. Recently, a non-parametric model of random uncertainties for reduced matrix models in structural dynamics was proposed by Soize (2000). The information used in this model does not require the description of the uncertain local parameters. This approach is based on a probability model for symmetric, positive definite random matrices deduced from the entropy optimization principle (Jaynes, 1957).

Here, the system's parameters, calibrated using experimental data, are modeled as random variables or processes which span a Hilbert space $\mathscr{H}_{\mathscr{G}}$. Assuming that the data are properly defined by a set of random variables $\{\xi(\theta)\}$, where θ belongs to the space of random events Ω, the state of the system, which is itself modeled as a random variable or process, lies in the Hilbert space $\mathscr{H}_{\mathscr{L}}$. A set of basis functions $\{\Psi\}$ of this space will be identified in the section dealing with polynomial chaos expansion (PCE). In order to isolate the random aspect of the problem, we will be using a decomposition of the assembly; therefore, let us present the reference problem on a decomposed structure.

2.1. Decomposition of an assembly

An assembly is composed of a set of *substructures* (each of which is a component of the assembly) which communicate with one another through *interfaces* (each interface representing a connection): see Fig. 1. Each interface is a mechanical entity with its own variables and its specific behavior which depends on the type of connection. Many different types of connections can be modeled by this approach, but in this paper we are considering only joints with a random elastic behavior. Two connected substructures are denoted with superscript E and E'. Each domain is designed by V^E (resp. $V^{E'}$) and their interface is designated by $\Gamma^{EE'}$.

The interface variables are two force fields $\vec{f}^E$ and $\vec{f}^{E'}$ and two dual displacement fields $\vec{w}^E$ and $\vec{w}^{E'}$ (Fig. 2). By convention, $\vec{f}^E$ and $\vec{f}^{E'}$ are the actions of the interface on the substructures and $\vec{w}^E$ and $\vec{w}^{E'}$ are the displacements of the substructures at the interface.

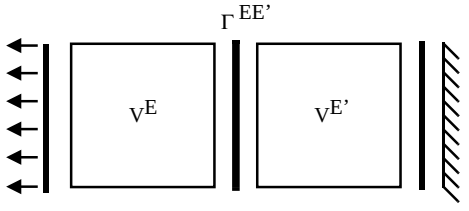

Fig. 1. Decomposition of an assembly.

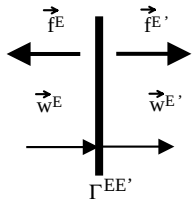

Fig. 2. Interface variables.

2.2. The problem in the substructures

We assume that the displacements and strains remain small during the evolution and, therefore, we make the assumption of small perturbations. The displacement field at any point M of V^E is a random field $\vec{u}^E(M,\theta)$; the associated space is $\mathscr{U}$. The strain field is $\epsilon(\vec{u}^E(M,\theta))$ and the current state of the structure is characterized by the stress field $\sigma^E(M,\theta)$.

The mechanical problem to be solved in each substructure is: find the displacement field $\vec{u}^E(M,\theta)$ and the stress field $\sigma^E(M,\theta)$ such that:

- Kinematic admissibility: $\forall M \in V^E$, $\forall \theta \in \Omega$

$$\epsilon = \epsilon(\vec{u}^E); \quad \vec{u}^E_{|\partial V^E} = \vec{w}^E \tag{1}$$

- Equilibrium: $\forall \vec{u}^\star \in \mathscr{U}$, $\forall \theta \in \Omega$

$$\int_{V^E} Tr(\sigma^E \epsilon(\vec{u}^\star))\,\mathrm{d}V^E - \int_{V^E} \vec{f}_{\mathrm{d}} \cdot \vec{u}^\star\,\mathrm{d}V - \int_{\partial V^E} \vec{f}^E \cdot \vec{u}^\star\,\mathrm{d}S = 0 \tag{2}$$

  where $\mathscr{U}$ is the set of finite-energy displacement fields on V^E, $\vec{u}^\star$ a virtual displacement field and $\vec{f}_{\mathrm{d}}$ a deterministic field of body forces.
- Elastic behavior: $\forall M \in V^E$, $\forall \theta \in \Omega$

$$\sigma^E = \mathbf{D}\epsilon(\vec{u}^E) \tag{3}$$

  where $\mathbf{D}$ is Hooke's operator, which, in our case, is deterministic.

2.3. The problem at the interfaces

The mechanical problem to be solved at each interface is: find the force fields ($\vec{f}^E(M,\theta)$ and $\vec{f}^{E'}(M,\theta)$) and the displacement fields ($\vec{w}^E(M,\theta)$ and $\vec{w}^{E'}(M,\theta)$) such that:

- Equilibrium: $\forall M \in \Gamma^{EE'}$, $\forall \theta \in \Omega$

$$\vec{f}^E(M,\theta) + \vec{f}^{E'}(M,\theta) = 0 \tag{4}$$

- Behavior: $\forall M \in \Gamma^{EE'}$, $\forall \theta \in \Omega$

$$\vec{f}^E(M,\theta) = \mathscr{R}(\vec{w}^{EE'}(M,\theta), \alpha(\theta)) \tag{5}$$

  where the behavior is expressed in the form of a behavior law $\mathscr{R}$ among the forces and a displacement jump across the interface $\vec{w}^{EE'}$ defined by:

$$\vec{w}^{EE'} = \vec{w}^{E'} - \vec{w}^{E} \tag{6}$$

and $\alpha(\theta)$ is a random material parameter. For example, a perfect connection between two substructures would be modeled as the following behavior:

$$\vec{w}^{EE'}(M,\theta) = 0 \tag{7}$$

In the case of random elastic conditions, the form of the behavior law $\mathscr{R}$ is:

$$\vec{f}^{E}(M,\theta) = \mathbf{k}(\alpha(\theta))\vec{w}^{EE'}(M,\theta) \tag{8}$$

where $\mathbf{k}$ is the interface's stiffness operator, which depends on a random material parameter $\alpha(\theta)$.

2.4. Discretization

Standard finite element discretization is used for the displacement field in the substructures:

$$\vec{u}^{E}(M,\theta) = \mathbf{N_s}(M)\mathbf{u}^{E}(\theta) \quad \text{and} \quad \epsilon(\vec{u}^{E}) = \mathbf{B}\mathbf{u}^{E}(\theta) \tag{9}$$

where $\mathbf{u}^{E}$ is the vector of nodal displacements and $\mathbf{N_s}$ are the classical finite element basis functions.

At the interfaces, a compatible discretization of the displacement fields is performed:

$$\vec{w}^{E}(M,\theta) = \mathbf{N_i}(M)\mathbf{w}^{E}(\theta) \quad \text{and} \quad \mathbf{w}^{EE'} = \mathbf{w}^{E'} - \mathbf{w}^{E} \tag{10}$$

where $\mathbf{N_i}$ are the finite element basis functions at the interfaces (Schellekens and De Borst, 1993).

2.5. Global resolution

When the reference problem described above is solved by classical global resolution, the interfaces are modeled by means of interface elements (Fig. 3). The nodal displacements at the interfaces $\mathbf{w}^{E}$ do not constitute additional variables, but are the restrictions of the substructure's displacements $\mathbf{u}^{E}$ at the boundary:

$$\mathbf{R}\mathbf{u}^{E}(\theta) = \mathbf{w}^{E}(\theta) \tag{11}$$

where $\mathbf{R}$ is the Boolean operator for the restriction at the interfaces. Then, the global problem is written as:

$$\mathbf{K}(\alpha(\theta))\mathbf{u}(\theta) = \mathbf{f} \tag{12}$$

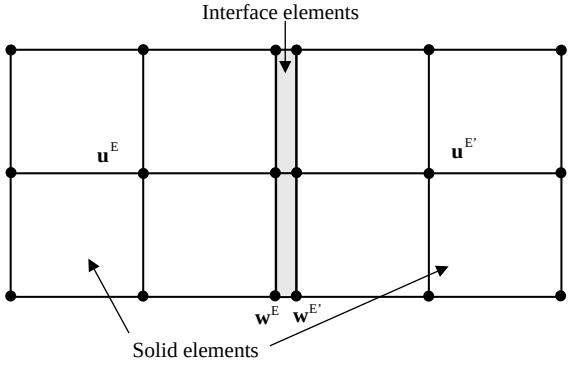

Fig. 3. Mesh used for global resolution.

where $\mathbf{u}(\theta)$ is the global vector of the nodal displacements and $\mathbf{f}$ is the deterministic vector of the nodal external forces. The global stiffness matrix $\mathbf{K}(\theta)$ is the assembly of the deterministic stiffness matrices of the substructures:

$$\mathbf{K}^E = \int_{V^E} \mathbf{B}^t \mathbf{D} \mathbf{B} \, \mathrm{d}V^E \tag{13}$$

and of the random stiffness matrices of the interfaces (Schellekens and De Borst, 1993):

$$\mathbf{K}^{EE'}(\alpha(\theta))$$

3. Polynomial chaos expansion (PCE)

Since the resolution process depends on the material properties of the interfaces, the nodal solution variables $\mathbf{u}(\theta)$ can be formally expressed as a non-linear functional of the set $\{\xi_j(\theta)\}$ used to represent the material's stochastic properties. It has been shown (Cameron and Martin, 1947) that this functional dependence can be expanded in terms of polynomial chaoses (P-C). Then, the truncated P-C expansion of the response takes the form:

$$\mathbf{u}(\theta) = \sum_{i=0}^{P} \mathbf{u}_i \Psi_i(\theta) \tag{14}$$

where $\{\Psi_i(\theta)\}$ are polynomials in the Gaussian random variables $\{\xi_i\}$. $\{\Psi_i(\theta)\}$ are Fourier–Hermite polynomials: they are orthogonal in the sense that their inner product $\langle \Psi_j \Psi_k \rangle$, which is defined as the statistical average of their product, is equal to $c_j \delta_{jk}$. Moreover, one can show that they constitute a complete basis in the space of second-order random variables. Therefore, once the *deterministic* nodal solutions $\mathbf{u}_i$ have been calculated, one obtains a complete probabilistic characterization of the process $\mathbf{u}(\theta)$. The number of polynomials (P) depends on the order p of the PCE and on the number L of stochastic parameters. The expressions of the polynomials used in this paper are given in Appendix A.

In the following sections, we will assume that the material parameters are constant throughout an interface. If they were not constant as well as non-deterministic, one could easily use a Karhunen–Loeve expansion to represent the spatial randomness of the interface's characteristics (Ghanem and Kruger, 1996).

4. The spectral stochastic finite element method

The random character of the material property α is made explicit by its argument θ. The stochastic material property $\alpha(\theta)$ is represented by:

$$\alpha(\theta) = \bar{\alpha}(1 + \delta\xi(\theta)) \tag{15}$$

where $\bar{\alpha}$ is the mathematical expectation of $\alpha(\theta)$, δ the coefficient of variation (standard deviation divided by the expectation) and $\xi(\theta)$ the standard normal random variable: $\xi(\theta) \sim N(0,1)$. For non-Gaussian material properties, the PCE is used to represent the material properties: the Gaussian process is a particular case chosen for the sake of simplicity (Ghanem, 1999). Following the traditional FE assembly procedure, this leads to the corresponding expansion of the stiffness matrix:

$$\mathbf{K} = \sum_{i=0}^{L} \xi_i \mathbf{K}_i \tag{16}$$

where $\mathbf{K_0}$ denotes the stiffness matrix for the mean material properties and the other terms correspond to the random fluctuations about the mean. The number of stochastic parameters is L. Expanding the nodal solution $\mathbf{u}(\theta)$ with respect to the polynomial chaos basis:

$$\mathbf{u}(\theta) = \sum_{j=0}^{P} \mathbf{u}_j \Psi_j(\theta) \tag{17}$$

and substituting Eqs. (16) and (17) into Eq. (12) leads to:

$$\sum_{j=0}^{P} \sum_{i=0}^{L} \xi_i \Psi_j(\theta) \mathbf{K}_i \mathbf{u}_j = \mathbf{f} \tag{18}$$

An equality, in a weak sense, can be derived by projecting Eq. (18) onto the subspace spanned by the polynomial chaos subset used in the approximation; this process results in the following equations:

$$\sum_{j=0}^{P} \sum_{i=0}^{L} \langle \xi_i \Psi_j(\theta) \Psi_k(\theta) \rangle \mathbf{K}_i \mathbf{u}_j = \langle \Psi_k(\theta) \rangle \mathbf{f}, \quad k = 0, 1, \ldots, P \tag{19}$$

The last equation can be rewritten as:

$$\sum_{j=0}^{P} \sum_{i=0}^{L} c_{ijk} \mathbf{K}_i \mathbf{u}_j = \delta_{0k} \mathbf{f}, \quad k = 0, 1, \ldots, P \tag{20}$$

where the coefficients c_{ijk} denote $\langle \xi_i \Psi_j(\theta) \Psi_k(\theta) \rangle$ and can be calculated only once. This system of linear equations must be solved for the unknown $\mathbf{u}_j$ of the PCE. The details of the above procedure were published in Ghanem and Spanos (1991). The implementation issues were addressed in a number of other references (Ghanem, 1999; Ghanem and Kruger, 1996). These equations can be assembled into a matrix of size $(P+1) \cdot n \times (P+1) \cdot n$ (n being the number of degrees of freedom) of the form:

$$\begin{pmatrix} \mathbf{K}^{(00)} & \mathbf{K}^{(01)} & \cdots & \cdots & \mathbf{K}^{(0P)} \\ \cdot & \cdot & \cdots & \cdots & \cdot \\ \cdot & \cdot & \mathbf{K}^{(jk)} & \cdots & \cdot \\ \cdot & \cdot & \cdots & \cdots & \cdot \\ \mathbf{K}^{(P0)} & \mathbf{K}^{(P1)} & \cdots & \cdots & \mathbf{K}^{(PP)} \end{pmatrix} \begin{pmatrix} \mathbf{u}_0 \\ \cdot \\ \mathbf{u}_k \\ \cdot \\ \mathbf{u}_P \end{pmatrix} = \begin{pmatrix} \mathbf{f}_0 \\ \cdot \\ 0 \\ \cdot \\ 0 \end{pmatrix} \tag{21}$$

where

$$\mathbf{K}^{(jk)} = \sum_{i=0}^{L} \langle \xi_i \Psi_j(\theta) \Psi_k(\theta) \rangle \mathbf{K}_i \tag{22}$$

In summary, this approach consist of expanding the random response process about a basis of the Hilbert space of random variables and of calculating the coefficients of the expansion. The result is a convergent expansion of the response in terms of multidimensional orthogonal polynomials. Although the methodology used is becoming widespread, serious obstacles have been encountered, from a computational point of view, in practical implementations. In large and realistic problems, the methodology is either cumbersome or computationally intensive. Some numerical strategies, such as iterative algorithms, have been devised to overcome the numerical difficulties arising in this context (Pellissetti and Ghanem, 2000). The

proposed approach uses the localization of the random characteristics in order to solve this type of problem more efficiently.

5. A dedicated approach

5.1. Discretization for a mixed method

In order to avoid solving a large problem when polynomial expansion is being used, we are proposing a dedicated approach which separates the treatment of the substructures from that of the interfaces. Here, the interface equations are treated in a mixed manner. Thus, we introduce a finite element discretization of the forces:

$$\vec{f}^E(M,\theta) = \mathbf{N_i}(M)\mathbf{f}^E(\theta) \tag{23}$$

The discrete form of the problem becomes: find the solution

$$s = \sum_E s^E; \quad s^E = \{\mathbf{u}^E(\theta), \mathbf{w}^E(\theta), \mathbf{f}^E(\theta)\}$$

such that on each substructure, $\forall\theta \in \Omega$,

- Kinematic admissibility: (discrete form of Eq. (1))

$$\mathbf{R}\mathbf{u}^E(\theta) = \mathbf{w}^E(\theta) \tag{24}$$

  where $\mathbf{R}$ is the deterministic Boolean operator for the restriction at the interfaces.
- Equilibrium and elastic behavior: (discrete form of Eqs. (2) and (3))

$$\mathbf{K}^E\mathbf{u}^E(\theta) = \mathbf{h}\mathbf{f}^E(\theta) \tag{25}$$

  with $\mathbf{K}^E$ the classical FE stiffness matrix which is here deterministic (see Eq. (3)) and

$$\mathbf{h} = \int_{\Gamma^{EE'}} \mathbf{N_i^t}\mathbf{N_i}\,\mathrm{d}\Gamma$$

- Interface equilibrium: (discrete form of Eq. (4))

$$\mathbf{f}^E(\theta) + \mathbf{f}^{E'}(\theta) = 0 \tag{26}$$

- Interface behavior: (discrete form of Eq. (5))

$$\mathbf{f}^E(\theta) = \mathscr{R}(\mathbf{w}^{EE'}(\theta), \alpha(\theta)) \tag{27}$$

5.2. The LATIN method

To solve the problem, we use the LArge Time INcrement (LATIN) approach (Ladevèze, 1999). The LATIN approach is based on the idea of separating the difficulties in order not to have to solve a problem which is both global and random. The equations are split into two groups with two corresponding sets of solutions:

- the set $\mathscr{A}_\mathrm{d}$ of the solutions s^E to the *linear* deterministic equations related to the substructures (Eqs. (24) and (25));
- the set Γ of the solutions s^E to the *local* equations related to the interfaces (Eqs. (26) and (27), which may be non-deterministic equations).

The search for the overall solution (i.e. the intersection of the two sets) is conducted iteratively by constructing approximate solutions s which verify the two groups of equations alternatively over the whole time history. Thus, each iteration in the process consists of two stages:

the local stage: for $s_n \in \mathscr{A}_d$ known, find $\hat{s}$ such that:

$$\hat{s} \in \Gamma \quad \text{(interfaces)} \tag{28}$$

$$\hat{s} - s_n \in E^+ \quad \text{(search direction)} \tag{29}$$

the global stage: for $\hat{s} \in \Gamma$ known, find s_{n+1} such that:

$$s_{n+1} \in \mathscr{A}_d \quad \text{(substructures)} \tag{30}$$

$$s_{n+1} - \hat{s} \in E^- \quad \text{(search direction)} \tag{31}$$

In our particular case of linear deterministic elastic substructures, the internal solution (displacement $\mathbf{u}^E(\theta)$) can be easily calculated from the boundary values ($\mathbf{w}^E(\theta)$ and $\mathbf{f}^E(\theta)$). Therefore, from this point on, we will represent a solution s only by the force and displacement fields on both sides of an interface.

The search directions are chosen such that convergence of the algorithm is ensured (Ladevèze, 1999). These conjugate search directions depend on the scalar parameter k_0:

$$\hat{s} - s_n \in E^+ \equiv (\hat{\mathbf{f}}^E - \mathbf{f}_n^E) = k_0(\hat{\mathbf{w}}^E - \mathbf{w}_n^E) \tag{32}$$

$$s_{n+1} - \hat{s} \in E^- \equiv (\mathbf{f}_{n+1}^E - \hat{\mathbf{f}}^E) = -k_0(\mathbf{w}_{n+1}^E - \hat{\mathbf{w}}^E) \tag{33}$$

The resolution algorithm can be represented as shown in Fig. 4. The solution s to the problem is the intersection of the sets $\mathscr{A}_d$ and Γ.

The solution to the problem does not depend on the value of the parameter k_0. This parameter affects only the convergence rate of the algorithm. For the quasi-static cases which interest us here, k_0 is given by:

$$k_0 = \frac{E}{L_c} \tag{34}$$

where E is the average Young's modulus and L_c the largest dimension of the structure. An error indicator is used to control the convergence of the algorithm. This indicator is an energy measure of the distance between the two solutions s_n and $\hat{s}$. PCE is used to represent all the problem's variables:

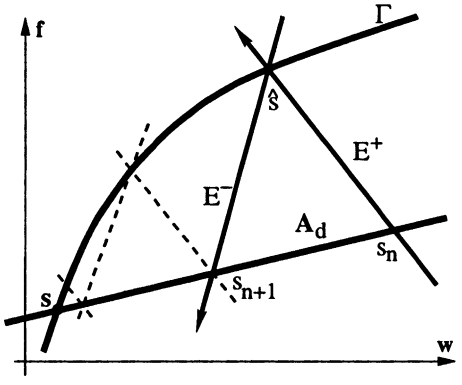

Fig. 4. The LATIN algorithm.

$$\mathbf{u}^E(\theta) = \sum_{i=0}^{P} \mathbf{u}_i^E \Psi_i(\theta) \tag{35}$$

$$\mathbf{w}_n^E(\theta) = \sum_{i=0}^{P} \mathbf{w}_{in}^E \Psi_i(\theta); \quad \hat{\mathbf{w}}^E(\theta) = \sum_{i=0}^{P} \hat{\mathbf{w}}_i^E \Psi_i(\theta) \tag{36}$$

$$\mathbf{f}_n^E(\theta) = \sum_{i=0}^{P} \mathbf{f}_{in}^E \Psi_i(\theta); \quad \hat{\mathbf{f}}^E(\theta) = \sum_{i=0}^{P} \hat{\mathbf{f}}_i^E \Psi_i(\theta) \tag{37}$$

For convenience, we note $\mathbf{w}^{EE'} = \mathbf{w}^E - \mathbf{w}^{E'}$ the jump of displacement at the interface:

$$\mathbf{w}_n^{EE'}(\theta) = \mathbf{w}_n^E(\theta) - \mathbf{w}_n^{E'}(\theta) = \sum_{i=0}^{P} (\mathbf{w}_{in}^E - \mathbf{w}_{in}^{E'}) \Psi_i(\theta) = \sum_{i=0}^{P} \mathbf{w}_{in}^{EE'} \Psi_i(\theta) \tag{38}$$

$$\hat{\mathbf{w}}^{EE'}(\theta) = \hat{\mathbf{w}}^E(\theta) - \hat{\mathbf{w}}^{E'}(\theta) = \sum_{i=0}^{P} (\hat{\mathbf{w}}_i^E - \hat{\mathbf{w}}_i^{E'}) \Psi_i(\theta) = \sum_{i=0}^{P} \hat{\mathbf{w}}_i^{EE'} \Psi_i(\theta) \tag{39}$$

5.3. Resolution of the local stage

At the local stage, the quantities $\mathbf{f}_n^E(\theta)$, $\mathbf{f}_n^{E'}(\theta)$, $\mathbf{w}_n^E(\theta)$ and $\mathbf{w}_n^{E'}(\theta)$ are known from the previous global stage. They are described by the coefficients of their chaos expansion: $\mathbf{f}_{in}^E$, $\mathbf{f}_{in}^{E'}$, $\mathbf{w}_{in}^E$ and $\mathbf{w}_{in}^{E'}$, $i = 0 \dots P$.

In the case of a random elastic interface, the problem which must be solved at the local stage is expressed by the following system.

$$\begin{cases} \hat{\mathbf{f}}^E(\theta) + \hat{\mathbf{f}}^{E'}(\theta) = 0 \\ \hat{\mathbf{f}}^E(\theta) = \mathbf{k}(\alpha(\theta)) \hat{\mathbf{w}}^{EE'}(\theta) \\ (\hat{\mathbf{f}}^E(\theta) - \mathbf{f}_n^E(\theta)) = k_0(\hat{\mathbf{w}}^E(\theta) - \mathbf{w}_n^E(\theta)) \\ (\hat{\mathbf{f}}^{E'}(\theta) - \mathbf{f}_n^{E'}(\theta)) = k_0(\hat{\mathbf{w}}^{E'}(\theta) - \mathbf{w}_n^{E'}(\theta)) \end{cases} \tag{40}$$

We assumed the stiffness to be constant along the interface. As mentioned in Section 3, if they were not constant as well as non-deterministic, one could easily use a Karhunen–Loeve expansion to represent the spatial randomness of the interface's characteristics (Ghanem and Kruger, 1996). Then, the problem is composed of a set of independent problems at each node of the interface. The interface's stiffness $\mathbf{k}$ consists of a normal stiffness and a tangential stiffness. The normal and tangential problems are uncoupled. Therefore, we are presenting only the resolution in one direction. We designate by $(\hat{f}^E, \hat{f}^{E'}, \hat{w}^{EE'} = \hat{w}^{E'} - \hat{w}^E)$ the unknowns at one node and in one direction. $(f_n^E, f_n^{E'}, w_n^E, w_n^{E'})$ are the associated variables known from the previous global stage. We assume that the behavior along the direction considered depends on a single random stiffness parameter $k_i(\theta)$. $i \in [1 \cdots L]$, L being the total number of random parameters.

Then, the problem is expressed in the form of the following scalar system:

$$\begin{cases} \hat{f}^E(\theta) + \hat{f}^{E'}(\theta) = 0 \\ \hat{f}^E(\theta) = k_i(\theta) \hat{w}^{EE'}(\theta) \\ (\hat{f}^E(\theta) - f_n^E(\theta)) = k_0(\hat{w}^E(\theta) - w_n^E(\theta)) \\ (\hat{f}^{E'}(\theta) - f_n^{E'}(\theta)) = k_0(\hat{w}^{E'}(\theta) - w_n^{E'}(\theta)) \end{cases} \tag{41}$$

where the random stiffness k_i is expressed according to Eq. (15):

$$k_i(\theta) = \bar{k}_i(1 + \delta\xi_i(\theta)) \tag{42}$$

System (41) reduces to the following equation:

$$(2k_i(\theta) + k_0)\hat{w}^{EE'}(\theta) = k_0(w_n^{E'}(\theta) - w_n^E(\theta)) - (f_n^{E'}(\theta) - f_n^E(\theta)) = \tilde{g}_n(\theta) \tag{43}$$

where the second member, denoted $\tilde{g}_n(\theta)$, is known from the previous global stage. The variables are expanded over the polynomial chaos.

$$\hat{w}^{EE'} = \sum_{j=0}^{P} \hat{w}_j^{EE'} \Psi_j(\theta) \quad \text{and} \quad \tilde{g}_n = \sum_{j=0}^{P} \tilde{g}_{jn} \Psi_j(\theta) \tag{44}$$

Eq. (43) becomes:

$$(2\bar{k}_i(1 + \delta\xi_i(\theta)) + k_0) \sum_{j=0}^{P} \hat{w}_j^{EE'} \Psi_j(\theta) = \sum_{j=0}^{P} \tilde{g}_{jn} \Psi_j(\theta) \tag{45}$$

A weak equality can be established by projecting this equation onto the subspace spanned by the polynomial chaos subset used in the approximation; this process results in the following equation:

$$(2\bar{k}_i + k_0) \sum_{j=0}^{P} \hat{w}_j^{EE'} c_{jk} + 2\bar{k}_i\delta \sum_{j=0}^{P} \hat{w}_j^{EE'} c_{ijk} = \sum_{j=0}^{P} \tilde{g}_{jn} c_{jk}, \quad k = 0, 1, \ldots, P \tag{46}$$

where $c_{ijk} = \langle \xi_i(\theta)\Psi_j(\theta)\Psi_k(\theta) \rangle$ and $c_{jk} = \langle \Psi_j(\theta)\Psi_k(\theta) \rangle$ (according to Eq. (20)).

Using the orthogonality properties of the basis functions, we obtain:

$$(2\bar{k}_i + k_0) c_{kk} \hat{w}_k^{EE'} + 2\bar{k}_i\delta \sum_{j=0}^{P} c_{ijk} \hat{w}_j^{EE'} = c_{kk} \tilde{g}_{kn}, \quad k = 0, 1, \ldots, P \tag{47}$$

and corresponds to a scalar system of size $(P + 1)$. Then, the remaining variables are calculated using the following system:

$$\begin{cases} \hat{f}_k^{E'} = -\hat{f}_k^E = \frac{1}{2}(k_0 \hat{w}_k^{EE'} + \tilde{g}_{kn}) \\ \hat{w}_k^E = w_{kn}^E + \frac{1}{k_0}(\hat{f}_k^E - f_{kn}^E) \\ \hat{w}_k^{E'} = w_{kn}^{E'} + \frac{1}{k_0}(\hat{f}_k^{E'} - \hat{f}_{kn}^{E'}) \end{cases}, \quad k = 0, 1, \ldots, P \tag{48}$$

Thus, the resolution of the local stage consists of solving a series of small independent systems of size $(P + 1)$ at each point and along each direction.

5.4. Resolution for the global stage

At the global stage, the quantities $\hat{\mathbf{f}}^E(\theta)$, $\hat{\mathbf{f}}^{E'}(\theta)$, $\hat{\mathbf{w}}^E(\theta)$ and $\hat{\mathbf{w}}^{E'}(\theta)$ are known from the previous local stage. They are described by the coefficients of their chaos expansion: $\hat{\mathbf{f}}_i^E$, $\hat{\mathbf{f}}_i^{E'}$, $\hat{\mathbf{w}}_i^E$, $\hat{\mathbf{w}}_i^{E'}$, $i \in [0 \cdots P]$.

At the global stage, the equilibrium equation (25), which also takes into account the search direction (Eq. (33)), becomes:

$$\mathbf{K}^E \mathbf{u}_{n+1}^E = \mathbf{h}(\hat{\mathbf{f}}^E - k_0(\hat{\mathbf{w}}_{n+1}^E - \hat{\mathbf{w}}^E)) \tag{49}$$

which, once kinematic admissibility (Eq. (24)) has been included, becomes:

$$[\mathbf{K}^E + k_0\mathbf{hR}]\mathbf{u}^E_{n+1} = \mathbf{h}(\hat{\mathbf{f}}^E + k_0\hat{\mathbf{w}}^E) \tag{50}$$

where $\tilde{\mathbf{K}}^E = [\mathbf{K}^E + k_0\mathbf{hR}]$ is a deterministic matrix.

Using the PCE (Eqs. (35)–(37)), we obtain:

$$\tilde{\mathbf{K}}^E \sum_{i=0}^{P} \mathbf{u}^E_{in+1} \Psi_i(\theta) = \sum_{i=0}^{P} \mathbf{h}(\hat{\mathbf{f}}^E_i + k_0\hat{\mathbf{w}}^E_i)\Psi_i(\theta) \tag{51}$$

where $\tilde{f}^E_i = \mathbf{h}(\hat{\mathbf{f}}^E_i + k_0\hat{\mathbf{w}}^E_i)$ on the right-hand side is known from the previous local stage. Since $\tilde{\mathbf{K}}^E$ is deterministic, a term-by-term identification of Eq. (51) leads to the following $(P+1)$ independent equations:

$$\tilde{\mathbf{K}}^E \mathbf{u}^E_{kn+1} = \tilde{f}^E_k, \quad k = 0, 1, \ldots, P \tag{52}$$

Once these independent problems have been solved, the boundary terms are calculated (kinematic admissibility (Eq. (24))):

$$\mathbf{w}^E_{in+1} = \mathbf{R}\mathbf{u}^E_{in+1}, \quad i = 0, 1, \ldots, P \tag{53}$$

The forces are obtained using the search direction (Eq. (33)):

$$\mathbf{f}^E_{in+1} = \hat{\mathbf{f}}^E_i - k_0(\mathbf{w}^E_{in+1} - \hat{\mathbf{w}}^E_i), \quad i = 0, 1, \ldots, P \tag{54}$$

It is important to observe that the matrices appearing in system Eq. (52) remain constant throughout the iterations and, therefore, need to be factorized only once before the first iteration. An even more important point is that the problems within the substructures are completely independent of one another and could be solved in parallel very efficiently.

6. 1D example: traction of two beams with an uncertain connection

In this section, we present a simple 1D example. We will derive the exact solution (Appendix B) and give the details of the SSFEM (Appendix C) and of our proposed approach (Appendix D). Let us consider the assembly of two substructures (each substructure being a beam with deterministic behavior) connected by an interface whose stiffness $k(\theta)$ is assumed to be random (Fig. 5).

The assembly is subjected to uniaxial tension. The only quantities used to represent the behavior of the beams are their respective tractional stiffness coefficients k_1 and k_2, which are derived from the material and geometric parameters:

$$k_i = \frac{E_i S_i}{L_i}, \quad i = 1, 2$$

where E_i is the Young's modulus, S_i the cross-section and L_i the length of the beam i.

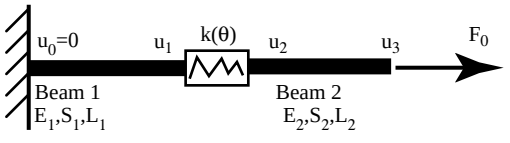

Fig. 5. The two beams connected by a random interface.

6.1. Convergence rate

The displacements converge rapidly toward the displacement calculated using the global method (Fig. 6).

6.2. Comparison of different methods

Fig. 7 presents the variation of the expectation and the variance of u_2 with respect to the coefficient of variation δ, as obtained respectively with the exact solution, the perturbation method, the direct SSFEM and the LATIN method. The LATIN method converges to the same solution as the direct SSFEM. The results of the perturbation method are valid only for small coefficients of variation, whereas the PCE (with order $p = 3$) is able to yield good results for larger values of the coefficient.

6.3. Cost comparison between the direct method and the iterative method

In order to compare the computational costs of the different strategies, we studied a 2D version of the previous 1D example. The behavior is still one-dimensional, but the 2D mesh makes it easy to vary the total number of degrees of freedom and the number of degrees of freedom at the interface. For the direct SSFEM resolution, we use a standard finite element solver: no special adaptation of the code was made to improve the efficiency of the resolution contrary to numerical strategies devised to overcome the numerical difficulties arising in this context (Pellissetti and Ghanem, 2000).

Fig. 8 shows the evolution of the computational costs of the direct SSFEM and of our proposed approach when the number of degrees of freedom increases. The order of the PCE is $p = 3$ and there is only one random variable, i.e. the number of functions in the expansion is 4 ($P = 3$). Our approach becomes much more efficient than the direct SSFEM when the number of degrees of freedom exceeds 1000.

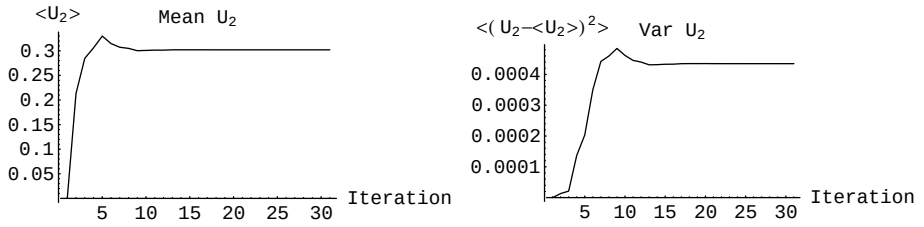

Fig. 6. Convergence for the mean and variance of the nodal displacement u_2.

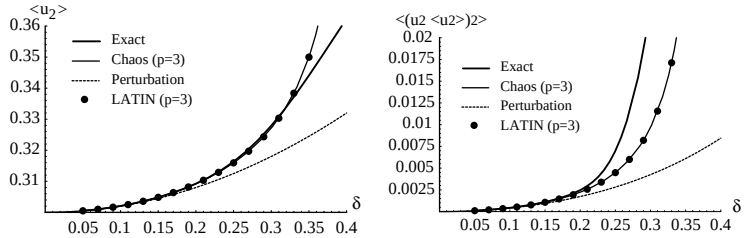

Fig. 7. Polynomial chaos: order $3\delta = 0.25$.

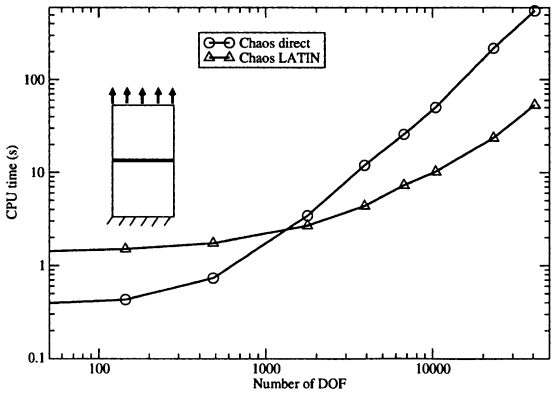

Fig. 8. Comparison between the direct and LATIN calculations: problem with a single interface (PC: Pentium III proc. 1.1 GHz, 512 MB RAM).

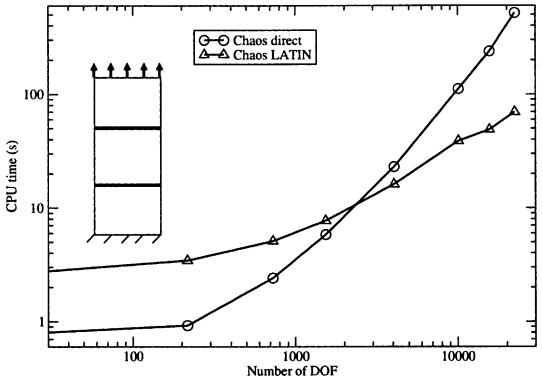

Fig. 9. Comparison between the direct and LATIN calculations: problem with two interfaces (PC: Pentium III proc. 1.1 GHz, 512 MB RAM).

Fig. 9 presents the same type of example, this time with two interfaces. In this case, the number of random variables is $L = 2$ and the order of the PCE is $p = 3$. Thus, there are 10 functions ($P = 9$) in the expansion (see Appendix A). The higher efficiency of the LATIN method is also observed on this example.

7. 2D example

Let us consider an assembly of three parts (Fig. 10) with two adhesively bonded joints (Tong and Steven, 1999; Van Straalen et al., 1998).

The dimensions, in millimeters, are shown in Fig. 10. The three parts have different material properties: the base (1) is made of cast iron ($E_1 = 120$ GPa, $\nu_1 = 0.3$), the L-shaped connecting part (2) of steel ($E_2 = 200$ GPa, $\nu_2 = 0.3$) and the vertical part (3) of aluminium ($E_3 = 70$ GPa, $\nu_3 = 0.3$). Part (3) is subjected to a vertical traction force $F = 250$ N. The quantities of interest are the displacement of point A at the top of part (3) and the maximum stresses in the bonded joints.

The adhesively bonded joints (denoted I and II in Fig. 10) are modeled by interfaces. The normal (k_n) and tangential (k_t) stiffness of each interface can be derived from the adhesive's characteristics:

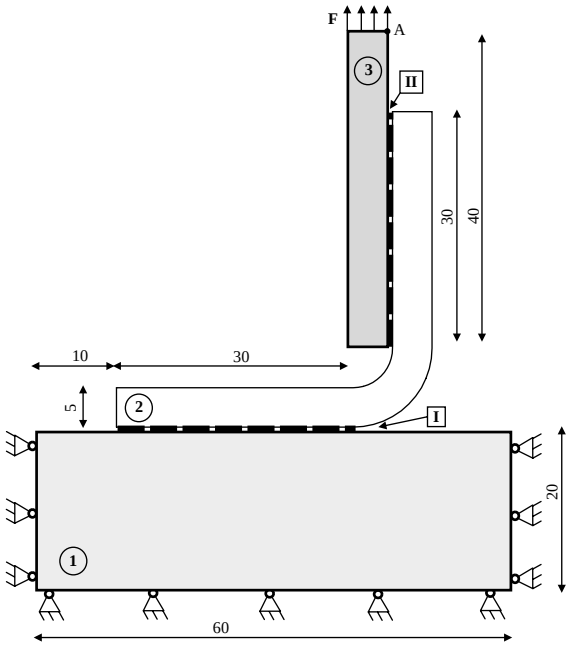

Fig. 10. The assembly with two bonded joints.

$$k_{\mathrm{n}} = \frac{E}{e}; \qquad k_{\mathrm{t}} = \frac{E}{2(1+v)e}$$

where E is the Young's modulus, v the Poisson's coefficient and e the thickness of the adhesive. The Young's modulus is assumed to be random:

$$E(\theta) = \overline{E}(1 + \delta\xi(\theta))$$

The two bonded joints (I and II) have the following characteristics:

$$\overline{E}_{\mathrm{I}} = 500 \text{ MPa}; \quad v_{\mathrm{I}} = 0.45; \quad e_{\mathrm{I}} = 0.3 \text{ mm}$$

$$\overline{E}_{\mathrm{II}} = 1000 \text{ MPa}; \quad v_{\mathrm{II}} = 0.45; \quad e_{\mathrm{II}} = 0.3 \text{ mm}$$

The mesh is composed of 17,820 four-node elements and contains 37,174 degrees of freedom.

Fig. 11 shows the probability density functions of the displacements at point A obtained by the LATIN method. These are compared to the solution obtained by a classical Monte Carlo method (10,000 draws). The results are very close. The LATIN results are the same as those obtained by direct resolution using the PCE.

Fig. 12 shows the convergence of the estimate of mean and variance obtained by the Monte Carlo method. They are compared to those obtained by the polynomial chaos method (fat dashed line). For a given accuracy, the number of draws is given asymptotically by the central limit theorem. For example, the estimate of U_x is given by:

$$\langle \widehat{U}_x \rangle = -0.02051 \pm \frac{0.0275n}{\sqrt{N}}$$

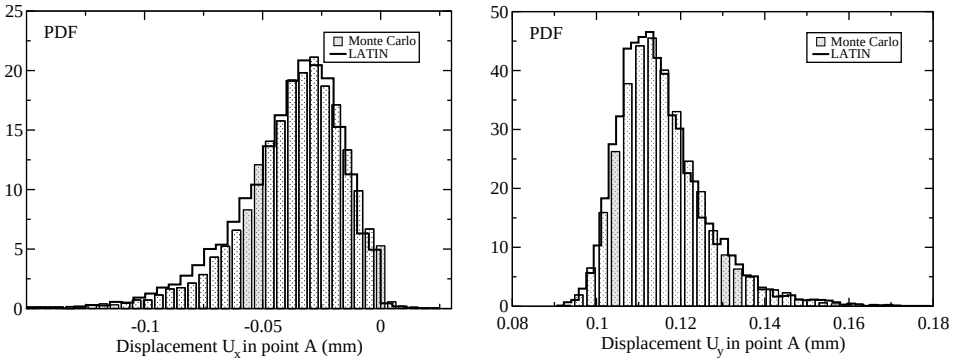

Fig. 11. Probability density functions of the displacements at point A ($\delta_{\mathrm{I}} = 0.2$ and $\delta_{\mathrm{II}} = 0.25$): comparison between the LATIN solution and the Monte Carlo solution (10,000 draws).

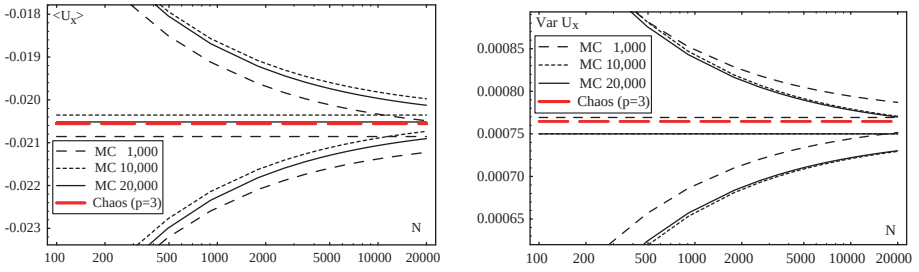

Fig. 12. Convergence of the mean and variance of the displacement U_x at point A ($\delta_{\mathrm{I}} = 0.2$ and $\delta_{\mathrm{II}} = 0.25$): comparison between the LATIN solution and the Monte Carlo solution for a confidence level of 0.95 ($n = 2$) for various sample sizes.

where $n = 2$ for a confidence level of 0.95 and N is the number of draws. We can notice the very good estimation by the polynomial chaos method both for the mean and the variance of U_x.

Table 1 compares the computational costs of the Monte Carlo method, the direct PCE and the LATIN method. One can appreciate how considerably shorter the computation time is using the LATIN method for this type of problem.

Fig. 13 shows the probability density functions of the maximum forces on the two interfaces. The construction of these functions requires no computational effort because the forces are explicit variables (represented using the PCE) in the LATIN resolution. These probability density functions were obtained using 20,000 Monte Carlo draws of the variable ξ.

Fig. 14 shows the evolutions of the expectation and standard deviation of the displacement U_y at point A when the coefficients of variation δ_{I} and δ_{II} vary between 0 (deterministic problem) and 0.4. One can observe that this displacement is influenced by the stochasticity of both interface variables but the influence

Table 1
Comparison of the computation costs on a PC (AMD Athlon proc. 1.4 GHz, 1.6 Gb RAM)

Calculation	CPU time (s)
Monte Carlo (10,000 draws)	75,700
Polynomial expansion—direct	780
Polynomial expansion—LATIN	185

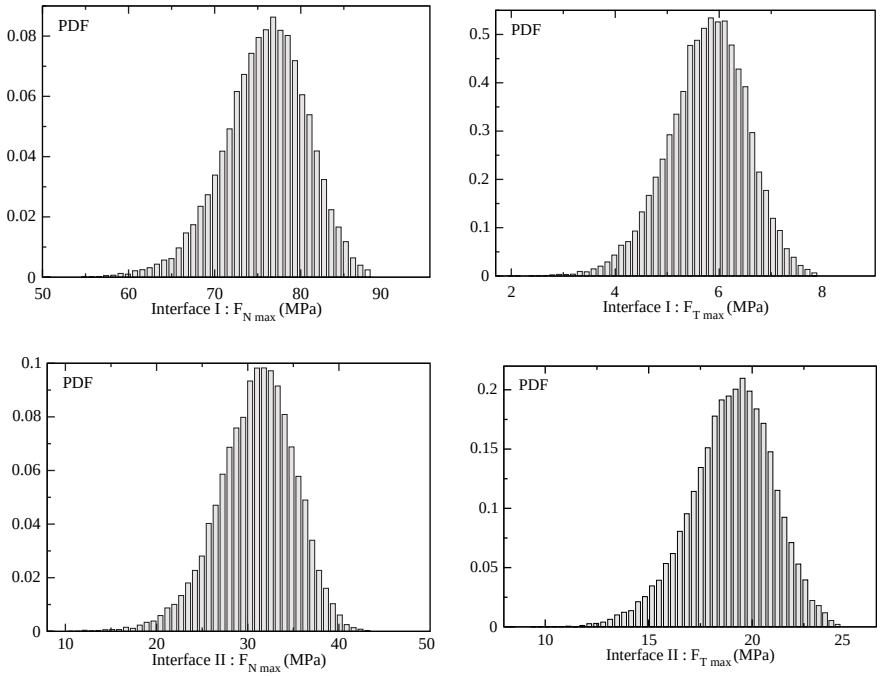

Fig. 13. Probability density functions of the maximum normal (F_N) and tangential (F_T) forces at the interfaces ($\delta_I = 0.2$ and $\delta_{II} = 0.25$).

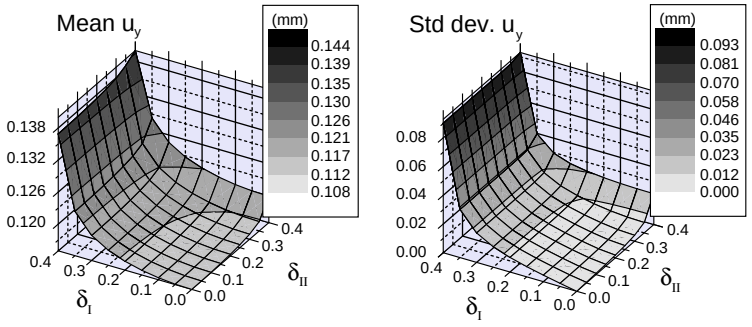

Fig. 14. Evolutions of the expectation and standard deviation of displacement U_y at point A with the coefficients of variation.

of the interface I is more significant because its stress type is dominating for the displacement at point A. Fig. 15 shows the evolutions of the expectation and standard deviation of the maximum normal force F_n at interface I when the coefficients of variation δ_I and δ_{II} vary between 0 and 0.4. Since the boundary conditions are expressed in terms of prescribed forces, one can observe that the stochasticity of the variable at interface II has nearly no influence upon the maximum forces at interface I: the forces applied on interface I remain nearly constant whatever the stiffness of interface II is.

As in the one-dimensional example (see Fig. 7), the results obtained by the LATIN method and by the direct SSFEM are the same. Therefore, they are not valid for large coefficients of variations as shown of the 1D example (Fig. 7).

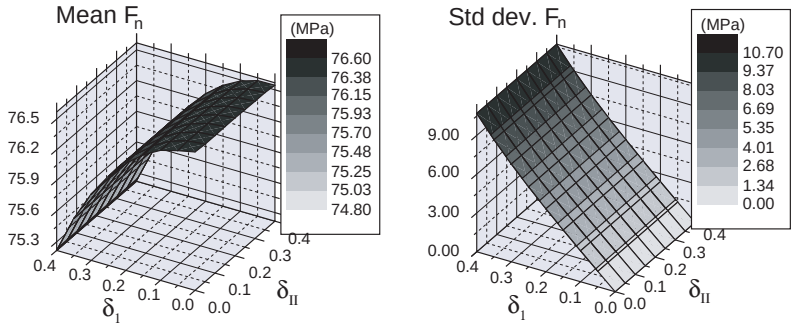

Fig. 15. Evolutions of the expectation and standard deviation of the maximum normal force F_n at interface I with the coefficients of variation.

8. Conclusions

We presented a computational strategy suitable for the calculation of the random response of assemblies of structures containing non-deterministic connections. This method is based on a decomposition of the assembly into substructures and interfaces. Our computational strategy, based on the LATIN method, allows the treatments of the random problem and of the global problem to be uncoupled. A polynomial chaos expansion is used to obtain the random solutions. The examples presented showed the numerical efficiency of the proposed approach compared to the Monte Carlo method and to the direct SSFEM for two-dimensional assemblies containing random elastic bonded joints.

Since the uncoupled treatments of the local and global problems lead to a drastic reduction in problem size, the numerical efficiency of the proposed approach can be very high. Another important point is that the linear systems for the substructures are independent of one another and could be solved in parallel very efficiently. The prolongation of this work will address non-linear interface behavior, such as contact and friction conditions.

Appendix A. Basis functions of the polynomial chaos expansion

Table 2 presents the expressions of the basis functions of the PCE for the orders $p = 0$–4 when only one random variable ξ is used ($L = 1$).

Table 3 presents the expressions of the basis functions of the PCE for the orders $p = 0$–3 when two random variables ξ_1 and ξ_2 are used ($L = 2$).

Appendix B. 1D example: the reference solution

In this particular case, an exact solution is available and can be used to check the accuracy of various numerical techniques. The characteristic equation of the uncertain interface is given by:

Table 2
One-dimensional polynomial chaoses and their variances ($L = 1$)

i	Ψ_i	$\langle \Psi_i^2 \rangle$	p
0	1	1	0
1	ξ	1	1
2	$-1 + \xi^2$	2	2
3	$\xi(-3 + \xi^2)$	6	3
4	$3 - 6\xi^2 + \xi^4$	24	4

Table 3
Two-dimensional polynomial chaoses and their variances ($L = 2$)

i	Ψ_i	$\langle \Psi_i^2 \rangle$	p
0	1	1	0
1	ξ_1	1	1
2	ξ_2	1	
3	$-1 + \xi_1^2$	2	2
4	$\xi_1\xi_2$	1	
5	$-1 + \xi_2^2$	2	
6	$\xi_1(-3 + \xi_1^2)$	6	3
7	$(-1 + \xi_1^2)\xi_2$	2	
8	$\xi_1(-1 + \xi_2^2)$	2	
9	$\xi_2(-3 + \xi_2^2)$	6	

$$k(\theta)(u_2(\theta) - u_1) = F_0 \quad \text{with } u_1 = \frac{F_0}{k_1} \tag{B.1}$$

$k(\theta)$ is the interface stiffness, which depends on a random material parameter $\xi(\theta)$. A standard normal distribution $\xi(\theta) \sim N(0,1)$ is chosen for ξ and δ represent the coefficient of variation according to Eq. (15).

$$k(\theta) = \bar{k}(1 + \delta\xi(\theta)) \quad \text{with } \langle \xi(\theta) \rangle = 0 \text{ and } \langle \xi(\theta)^2 \rangle = 1 \tag{B.2}$$

The displacement u_2 is an explicit function of the random variable ξ:

$$u_2 = g(\xi) = F_0\left(\frac{1}{k_1} + \frac{1}{\bar{k}(1 + \delta\xi)}\right) \quad \text{and} \quad \xi = g^{-1}(u_2)$$

The distribution of u_2 is known and its density function f_{u_2} is related to the density function f_ξ by the following equation:

$$f_{u_2}(u_2) = \frac{f_\xi(\xi)}{|\frac{\mathrm{d}g(\xi)}{\mathrm{d}\xi}|}$$

The expectation of u_2 is given by:

$$\langle u_2(\theta) \rangle = \bar{u}_2 = F_0\left(\frac{1}{k_1} + \frac{1}{\bar{k}}\langle Y \rangle\right) \quad \text{with } Y = \frac{1}{1 + \delta\xi}$$

and the standard deviation of u_2 by:

$$\langle (u_2(\theta) - \bar{u}_2)^2 \rangle = \left(\frac{F_0}{\bar{k}}\right)^2 \langle (Y - \langle Y \rangle)^2 \rangle$$

Fig. 16 presents the density function f_ξ of the standard normal variable $\xi(\theta)$ and the density function f_{u_2} of the displacement u_2. The Monte Carlo results (10,000 draws) for the two variables are also presented on the same figure.

Appendix C. 1D example: direct resolution using the polynomial chaos expansion

Let us interpolate the displacement $u(x,\theta)$ between the nodal displacement vector $\mathbf{u}(\theta)$ and the shape function vector $\mathbf{N}(x)$:

$$u(x,\theta) = \sum_{i=1}^{n} N_i(x)u_i(\theta) = \mathbf{N}(x)\mathbf{u}(\theta)$$

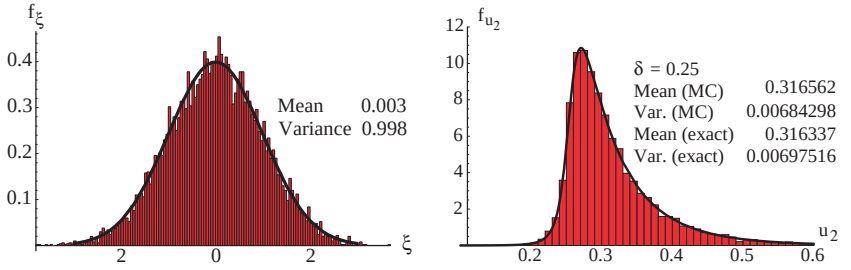

Fig. 16. Exact probability density functions f_ξ and f_{u_2} and the corresponding Monte Carlo results.

By applying the strain–displacement relationship, we obtain:

$$[(\mathbf{K_0} + \xi(\theta)\mathbf{K_1})]\mathbf{u}(\theta) = \mathbf{f} \tag{C.1}$$

The stiffness matrices $\mathbf{K_0}$ and $\mathbf{K_1}$, obtained from the element stiffness matrices, are given by:

$$\mathbf{K_0} = \begin{pmatrix} k_1 + \bar{k} & -\bar{k} & 0 \\ -\bar{k} & k_2 + \bar{k} & -k_2 \\ 0 & -k_2 & k_2 \end{pmatrix}; \qquad \mathbf{K_1} = \begin{pmatrix} \bar{k}\delta & -\bar{k}\delta & 0 \\ -\bar{k}\delta & \bar{k}\delta & 0 \\ 0 & 0 & 0 \end{pmatrix}$$

$\mathbf{u}(\theta)$ is the global vector of the unknown nodal displacements and $\mathbf{f}$ is the deterministic vector of the external forces:

$$\mathbf{u}(\theta) = [\, u_1(\theta) \quad u_2(\theta) \quad u_3(\theta) \,]^{\mathrm{T}}; \qquad \mathbf{f} = [\, 0 \quad 0 \quad F_0 \,]^{\mathrm{T}}$$

The PCE of order $p = 3$ ($P = 3$, see Appendix A) yields:

$$\mathbf{u}(\theta) = \sum_{i=0}^{3} \mathbf{u_i} \Psi_i(\theta) \tag{C.2}$$

The vectors $\mathbf{u_i}$ represent the magnitude of the projections of the nodal displacement vector $\mathbf{u}(\theta)$ onto the spaces spanned by the successive polynomial chaoses $\Psi_i(\theta)$. The dimension of each $\mathbf{u_i}$ correspond of the number of dof of the deterministic finite element problem. Eq. (C.2) leads to the following global linear system (equivalent to system Eq. (21)):

$$\begin{bmatrix} \mathbf{K_0} & \mathbf{K_1} & 0 & 0 \\ \mathbf{K_1} & \mathbf{K_0} & 2\mathbf{K_1} & 0 \\ 0 & 2\mathbf{K_1} & 2\mathbf{K_0} & 6\mathbf{K_1} \\ 0 & 0 & 6\mathbf{K_1} & 6\mathbf{K_0} \end{bmatrix} \begin{bmatrix} \mathbf{u_0} \\ \mathbf{u_1} \\ \mathbf{u_2} \\ \mathbf{u_3} \end{bmatrix} = \begin{bmatrix} \mathbf{f} \\ 0 \\ 0 \\ 0 \end{bmatrix}$$

The statistical moments can be obtained directly from the polynomial chaos representation of the solution.

The mean response vector is given by:

$$\langle \mathbf{u}(\theta) \rangle = \mathbf{u}_0$$

and the covariance matrix $\mathbf{R_{uu}}$ of the response by:

$$\mathbf{R_{uu}} = \langle (\mathbf{u} - \langle \mathbf{u} \rangle)(\mathbf{u} - \langle \mathbf{u} \rangle)^{\mathrm{H}} \rangle = \sum_{i=1}^{3} \langle \Psi_i^2(\xi(\theta)) \rangle \mathbf{u_i} \mathbf{u_i}^{\mathrm{H}}$$

where superscript H denotes hermitian transpose.

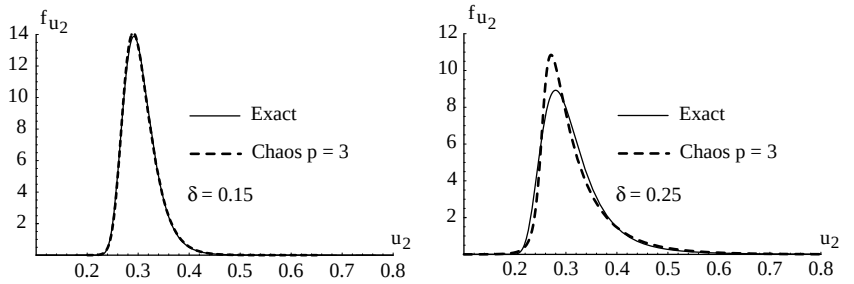

Fig. 17. Density function f_{u_2} for $\delta = 0.15$ and 0.25 (expansion order $p = 3$).

Fig. 17 presents the results of the calculation of the density function f_{u_2} for two different values of the coefficient of variation δ using the SSFEM. These results are compared with the exact solution. When the coefficient of variation is relatively small ($\delta = 0.15$), the SSFEM gives an almost exact solution. For a larger value of the coefficient ($\delta = 0.25$), the SSFEM solution is less accurate. The complete comparison is shown in Fig. 7.

Appendix D. 1D example: LATIN method

We will merely review the main equations of the two stages of the LATIN method for this simple 1D example.

D.1. Local stage: the interface with a random stiffness

We must solve Eq. (43)

$$(2k(\theta) + k_0)(\hat{u}_2(\theta) - \hat{u}_1(\theta)) = \tilde{g}_n(\theta) \tag{D.1}$$

The variables are expanded over the polynomial chaos:

$$(\hat{u}_2(\theta) - \hat{u}_1(\theta)) = \hat{u}^{12}(\theta) = \sum_{j=0}^{P} \hat{u}_j^{12} \Psi_j(\theta) \quad \text{and} \quad \tilde{g}_n = \sum_{j=0}^{P} \tilde{g}_{jn} \Psi_j(\theta) \tag{D.2}$$

If the order of the PCE is $p = 3$, the size of the linear scalar system to be solved is $(P + 1) = 4$:

$$\begin{bmatrix} a & b & 0 & 0 \\ b & a & 2b & 0 \\ 0 & 2b & 2a & 6b \\ 0 & 0 & 6b & 6a \end{bmatrix} \begin{bmatrix} \hat{u}_0^{12} \\ \hat{u}_1^{12} \\ \hat{u}_2^{12} \\ \hat{u}_3^{12} \end{bmatrix} = \begin{bmatrix} \tilde{g}_{0n} \\ \tilde{g}_{1n} \\ \tilde{g}_{2n} \\ \tilde{g}_{3n} \end{bmatrix} \quad (a = k_0 + 2\bar{k};\ b = 2\bar{k}\delta)$$

Then, the remaining variables are calculated from the system Eq. (48):

$$\begin{cases} \hat{f}_k^2 = -\hat{f}_k^1 = \frac{1}{2}(k_0 \hat{u}_k^{12} + \tilde{g}_{kn}) \\ \hat{u}_k^1 = u_{kn}^1 + \frac{1}{k_0}(\hat{f}_k^1 - f_{kn}^1) \\ \hat{u}_k^2 = u_{kn}^2 + \frac{1}{k_0}(\hat{f}_k^2 - f_{kn}^2) \end{cases} \quad , \quad k = 0, \ldots, 3$$

D.2. Resolution for the global stage

All the quantities $\hat{f}$ and $\hat{u}$ are known from the previous local stage. The system Eq. (52) must be solved for each substructure i:

$$\left[\begin{pmatrix} k_i & -k_i \\ -k_i & k_i \end{pmatrix} + \begin{pmatrix} k_0 & 0 \\ 0 & k_0 \end{pmatrix}\right]\begin{bmatrix} u_{in}^1 \\ u_{in}^2 \end{bmatrix} = \begin{bmatrix} \hat{f}_i^1 + k_0\hat{u}_i^1 \\ \hat{f}_i^2 + k_0\hat{u}_i^1 \end{bmatrix}$$

Therefore, for each substructure, one must perform $P+1=4$ resolutions of 2×2 small systems with $P+1$ right-hand sides. Let us remember that the matrices remain constant throughout the iterations. Once these independent problems have been solved, the boundary terms are calculated (Eq. (53)) and the forces are obtained using the search direction (Eq. (54)).

References

Blanzé, C., Champaney, L., Cognard, J., Ladevèze, P., 1995. A modular approach to structure assembly computations. Application to contact problems. Eng. Comput. 13 (1), 15–32.

Blanzé, C., Champaney, L., Védrine, P., 2000. Contact problems in the design of a superconducting quadrupole prototype. Eng. Comput. 17 (2–3), 136–153.

Cameron, R., Martin, W., 1947. The orthogonal development of non linear functionals in series of Fourier–Hermite functionals. Ann. Math. 48 (16), 385–392.

Deb, M.K., Babuska, I.M., Oden, J.T., 2001. Solution of stochastic partial differential equations using galerkin finite element techniques. Comput. Methods Appl. Mech. Eng. 190 (1–4), 6359–6372.

Elishakoff, I., Ren, Y., 1999. The bird's eye view on finite element method for structures with large stochastic variations. Comput. Methods Appl. Mech. Eng. 168 (1–4), 51–61.

Ghanem, R., 1999. Ingredients for a general purpose stochastic finite elements implementation. Comput. Methods Appl. Mech. Eng. 168, 19–34.

Ghanem, R., Brzakala, W., 1996. Stochastic finite-element analysis of soil layers with random interface. J. Eng. Mech., ASCE 122 (4), 361–369.

Ghanem, R., Kruger, R., 1996. Numerical solutions of spectral stochastic finite element systems. Comput. Methods Appl. Mech. Eng. 129, 289–303.

Ghanem, R., Spanos, P., 1991. Stochastic Finite Elements: A Spectral Approach. Springer, Berlin.

Jaynes, E., 1957. Information theory and statistical mechanics. Phys. Rev. 106 (4), 620–630.

Kleiber, M., Hien, T., 1992. The Stochastic Finite Element Method. Basic Perturbation Technique and Computer Implementation. John Willey & Sons.

Ladevèze, P., 1999. Nonlinear Computational Structural Mechanics—New Approaches and Non-Incremental Methods of Calculation. Springer-Verlag.

Ladevèze, P., Guitard, L., Champaney, L., Aubard, X., 2000. Debond modeling for multidirectional composites. Comput. Methods. Appl. Mech. Eng. 185, 109–122.

Lin, Y., Kozin, F., Wen, Y., Casciati, F., Schueller, G., Kiureghian, A.D., Ditlevsen, O., Vanmarcke, E., 1986. Methods of stochastic structural dynamics. Struct. Safety 3, 167–194.

Loeve, M., 1977. Probability Theory, fourth ed. Springer, New York.

Matthies, H.G., Brenner, C.E., Bucher, C.G., Guedes Soares, C., 1997. Uncertainties in probabilistic numerical analysis of structures and solids—stochastic finite elements. Struct. Safety 19 (3), 283–336.

Pellissetti, M., Ghanem, R., 2000. Iterative solution of systems of linear equations arising in the context of the stochastic fem. J. Adv. Eng. Software 31, 607–616.

Schellekens, J., De Borst, R., 1993. On the numerical integration of interface elements. Int. J. Numer. Meth. Eng. 36, 43–66.

Soize, C., 2000. A nonparametric model of random uncertainties for reduced matrix models in structural dynamics. Probabil. Eng. 15 (3), 277–294.

Tong, L., Steven, G., 1999. Analysis and Design of Structural Bonded Joints. Kluwer Academic Publisher, Dordrecht.

Van Straalen, I., Wardenier, J., Vogelesang, L., Soetens, F., 1998. Structural adhesive bonded joints in engineering—drafting design rules. Int. J. Adhes. Adhes. 18, 41–49.

Vanmarcke, E., 1983. Random Fields: Analysis and Synthesis. The MIT Press, Cambridge, MA.

Vanmarcke, E., Shinozuka, M., Nakagiri, S., Schueller, G., Grigoriu, M., 1988. Randoms fields and stochastic finite elements. J. Struct. Safety, 143–166.
Wiener, N., 1938. The homogeneous chaos. Am. J. Math. 60, 897–936.